

# A basis-set based Fortran program to solve the Gross-Pitaevskii Equation for dilute Bose gases in harmonic and anharmonic traps

Rakesh Prabhat Tiwari<sup>1,2</sup>, Alok Shukla<sup>3</sup>

*Physics Department, Indian Institute of Technology, Powai, Mumbai 400076,  
INDIA*

---

## Abstract

Inhomogeneous boson systems, such as the dilute gases of integral spin atoms in low-temperature magnetic traps, are believed to be well described by the Gross-Pitaevskii equation (GPE). GPE is a nonlinear Schrödinger equation which describes the order parameter of such systems at the mean field level. In the present work, we describe a Fortran 90 computer program developed by us, which solves the GPE using a basis set expansion technique. In this technique, the condensate wave function (order parameter) is expanded in terms of the solutions of the simple-harmonic oscillator (SHO) characterizing the atomic trap. Additionally, the same approach is also used to solve the problems in which the trap is weakly anharmonic, and the anharmonic potential can be expressed in a polynomial in the position operators  $x$ ,  $y$ , and  $z$ . The resulting eigenvalue problem is solved iteratively using either the self-consistent-field (SCF) approach, or the imaginary time steepest-descent (SD) approach. Iterations can be initiated using either the simple-harmonic-oscillator ground state solution, or the Thomas-Fermi (TF) solution. It is found that for condensates containing up to a few hundred atoms, both approaches lead to rapid convergence. However, in the strong interaction limit of condensates containing thousands of atoms, it is the SD approach coupled with the TF starting orbitals, which leads to quick convergence. Our results for harmonic traps are also compared with those published by other authors using different numerical approaches, and excellent agreement is obtained. GPE is also solved for a few anharmonic potentials, and the influence of anharmonicity on the condensate is discussed. Additionally, the notion of Shannon entropy for the condensate wave function is defined and studied as a function of the number of particles in the trap. It is demonstrated numerically that the entropy increases with the particle number in a monotonic way.

*Key words:* Bose-Einstein condensation, Gross-Pitaevskii Equation  
Anharmonic potential, Numerical Solutions

*PACS:* 02.70.-c, 02.70.Hm, 03.75.Hh, 03.75.Nt

---

## Program Summary

*Title of program:* bose.x

*Catalogue Identifier:*

*Program summary URL:*

*Program obtainable from:* CPC Program Library, Queen's University of Belfast, N. Ireland

*Distribution format:* tar.gz

*Computers :* PC's/Linux, Sun Ultra 10/Solaris, HP Alpha/Tru64, IBM/AIX

*Programming language used:* mostly Fortran 90

*Number of bytes in distributed program, including test data, etc.:* size of the tar file 153600 bytes

*Number of lines in distributed program, including test data, etc.:* lines in the tar file 4221

*Card punching code:* ASCII

*Nature of physical problem:* It is widely believed that the static properties of dilute Bose condensates, as obtained in atomic traps, can be described to a fairly good accuracy by the time-independent Gross-Pitaevskii equation. This program presents an efficient approach of solving this equation.

*Method of Solution:* The solutions of the Gross-Pitaevskii equation corresponding to the condensates in atomic traps are expanded as linear combinations of simple-harmonic oscillator eigenfunctions. Thus, the Gross-Pitaevskii equation which is a second-order nonlinear differential equation, is transformed into a matrix eigenvalue problem. Thereby, its solutions are obtained in a self-consistent manner, using methods of computational linear algebra.

*Unusual features of the program:* None

## 1 Introduction

Ever since the discovery of Bose-Einstein condensation (BEC) in dilute atomic gases[1,2,3], theoretical studies of this and related phenomenon in such systems have grown exponentially[4]. For most of the theoretical studies of BEC in dilute gases, the starting point is the so-called Gross-Pitaevskii equation (GPE)[5,6], which is nothing but a mean-field Schrödinger equation for a system of Bosons interacting through a two-body interaction described by  $\delta$ -function. In all but the simplest of the cases, one needs to solve the GPE using numerical methods. For problems involving the static properties of the

---

<sup>1</sup> Done in partial fulfillment of the requirements for the degree of Bachelor of Technology at the Indian Institute of Technology, Bombay.

<sup>2</sup> Present address: Department of Physics, The Ohio State University, Columbus, OH 43210, USA. email:tiwari.12@osu.edu

<sup>3</sup> Author to whom all the correspondence should be addressed. email:shukla@phy.iitb.ac.in

condensate, the numerical solutions of the time-independent GPE are of interest. And, indeed, over last several years, a significant amount of work has been performed towards developing novel approaches and algorithms meant for solving both time-dependent and independent GPE. Next we survey some of the recent literature in the field, restricting ourselves to the methods aimed at solving the time-independent GPE, which is the subject of the present paper. Edwards and Burnett developed a Runge-Kutta method based finite difference approach for solving the time-independent GPE for spherical condensates[7]. In another paper Edwards *et al.* used the basis set approach similar to the one presented here, to solve the GPE for anisotropic traps[8]. Dalfovo and Stringari developed a finite-difference based method for solving the time-independent GPE both for the ground state, and the vortex states, in anisotropic traps[9]. Esry used a finite-element approach to solve for the both the time-independent GPE, as well as, the Hartree-Fock equations for bosons confined in anisotropic traps[10]. Schneider and Feder used a discrete variable representation (DVR), coupled with a Gaussian quadrature integration scheme, to obtain the ground and the excited states of GPE in three dimensions[11]. Adhikari used a finite-difference based approach to solve the two-dimensional time-independent GPE[12,13]. Tosi and coworkers developed finite-difference, and imaginary-time, approach for solving the time-independent GPE[14]. Recently, Bao and Tang developed a novel scheme for obtaining the ground state of the GPE, by directly minimizing the corresponding energy functional[15]. Additionally, utilizing harmonic oscillator basis set, and Gauss-Hermite quadrature integration scheme, Dion and Cancès have proposed a scheme for solving both the time-dependent and -independent GPE[16]. Earlier, we had also proposed an alternative scheme for dealing with condensates with a large number of particles, and high number densities[17].

In this paper, we describe a Fortran program developed by us which solves time-independent GPE corresponding to bosons trapped in Harmonic traps. Instead of using the more common finite-difference approach, we have chosen the basis-set based approach popular in quantum chemistry[18]. The basis set chosen for this case is the Cartesian simple-harmonic-oscillator (SHO) basis set. The choice of a Cartesian basis set allows us to treat the cases ranging from spherical condensates to completely anisotropic condensates on an equal footing. Additionally, using the same approach our program allows to solve the time-independent GPE for anharmonic traps as well provided the anharmonic term can be expressed as a polynomial in various powers of coordinates  $x$ ,  $y$ , and  $z$ . As far as the SCF solution of the GPE is concerned, our program allows both the matrix-diagonalization based scheme, as well as the use of the imaginary-time steepest-descent method. Our program also allows the user to initiate the SCF process using either the SHO ground state orbital, or the Thomas-Fermi solution. We present the results of the calculations performed with our code for several interesting cases, and very good agreement is obtained with the existing results in the literature. Additionally, in the present

paper we have defined the notion of Shannon entropy in the context of GPE, and presented various quantitative calculations of the quantity.

Remainder of the paper is organized as follows. In the next section we discuss the basic theoretical aspects of our approach. Next, in section 3, we briefly describe the most important subroutines that comprise our program. In section 4 we provide detailed explanation about installing and compiling our program. Additionally, in the same section we explain how to prepare an input file, and describe the contents of a typical output file. In section 5 we discuss the convergence properties of the program with respect to the: (a) size of the basis set, and (b) the method of solution. In section 6, we discuss results of several example runs of our program, and compare them to those published earlier. Additionally, in the same section, we present our results on the Shannon entropy of the condensate, and on the solutions obtained in the presence of various anharmonic potentials. Finally, in section 7, we present our conclusions. In the Appendix we present the derivation of an analytical formula which we have used in our program to compute the two-particle interaction integrals.

## 2 Theory

For the present case, the time-independent Gross-Pitaevskii equation is

$$\left(-\frac{\hbar^2}{2m}\nabla^2 + V_{\text{ext}}(\mathbf{r}) + \frac{4\pi\hbar^2aN}{m}|\psi(\mathbf{r})|^2\right)\psi(\mathbf{r}) = \mu\psi(\mathbf{r}), \quad (1)$$

where  $\psi(\mathbf{r})$  is condensate wave function one is solving for,  $V_{\text{ext}}(\mathbf{r}) = \frac{1}{2}m(\omega_x^2x^2 + \omega_y^2y^2 + \omega_z^2z^2) + V^{\text{anh}}(x, y, z)$  is the confining potential for a general anisotropic trap ( $\omega_i$ 's are the trap frequencies) with the anharmonic term  $V^{\text{anh}}(x, y, z)$ ,  $a$  is the s-wave scattering length characterizing the two-body interactions among the atoms,  $N$  is the total number of bosons in the condensate, and  $\mu$  is the chemical potential. We are assuming that the condensate wave function is normalized to unity. Before attempting numerical solutions of Eq. (1), we cast it in a dimensionless form by making the transformations[15]

$$\tilde{\mathbf{r}} = \frac{\mathbf{r}}{a_x} \quad (2a)$$

$$\tilde{\psi}(\tilde{\mathbf{r}}) = a_x^{3/2}\psi(\mathbf{r}) \quad (2b)$$

where  $a_x = \sqrt{\frac{\hbar}{m\omega_x}}$  is the ‘‘harmonic oscillator length’’ in the  $x$  direction. This finally leads to the dimensionless form of the GPE

$$\left(-\frac{1}{2}\tilde{\nabla}^2 + V_{\text{ext}}(\tilde{\mathbf{r}}) + \kappa|\tilde{\psi}(\tilde{\mathbf{r}})|^2\right)\tilde{\psi}(\tilde{\mathbf{r}}) = \tilde{\mu}\tilde{\psi}(\tilde{\mathbf{r}}), \quad (3)$$

where  $\tilde{\mu}$  is the chemical potential in the units of  $\hbar\omega_x$ ,  $\kappa = \frac{4\pi Na}{a_x}$  is a dimensionless constant determining the strength of the two-body interactions in the gas, and for the harmonic oscillator potential  $V_{\text{ext}}(\tilde{\mathbf{r}}) = \frac{1}{2}(\tilde{x}^2 + \gamma_y^2\tilde{y}^2 + \gamma_z^2\tilde{z}^2) + V^{\text{anh}}(\tilde{x}, \tilde{y}, \tilde{z})$ , with  $\gamma_y = \frac{\omega_y}{\omega_x}$  and  $\gamma_z = \frac{\omega_z}{\omega_x}$  being the two aspect ratios. We will now discuss the basis-set expansion technique, used for solving the GPE[8,11,16]. In this approach, one expands  $\tilde{\psi}(\tilde{\mathbf{r}})$  as a linear combination of basis functions of three-dimensional anisotropic simple harmonic oscillator

$$\tilde{\psi}(\tilde{\mathbf{r}}) = \sum_{i=1}^{N_{\text{basis}}} C_i \Phi_i(\tilde{x}, \tilde{y}, \tilde{z}) = \sum_{i=1}^{N_{\text{basis}}} C_i \phi_{n_{xi}}(\tilde{x}) \phi_{n_{yi}}(\tilde{y}) \phi_{n_{zi}}(\tilde{z}), \quad (4)$$

where  $\phi_{n_{xi}}(\tilde{x})$ ,  $\phi_{n_{yi}}(\tilde{y})$ , and  $\phi_{n_{zi}}(\tilde{z})$ , are the harmonic oscillator basis functions corresponding to  $x$ ,  $y$ , and  $z$  directions, respectively,  $C_i$  is the expansion coefficient, and  $N_{\text{basis}}$  is the total number of basis functions used. In dimensionless units, *e.g.*,  $\phi_{n_{zi}}(\tilde{z})$  can be written as

$$\phi_{n_{zi}}(\tilde{z}) = \left(\frac{\gamma_z}{\pi}\right)^{1/4} \frac{1}{\sqrt{2^{n_{zi}} n_{zi}!}} H_{n_{zi}}(\tilde{z}\sqrt{\gamma_z}) \exp\left(-\frac{\gamma_z \tilde{z}^2}{2}\right), \quad (5)$$

where  $H_{n_{zi}}(\tilde{z}\sqrt{\gamma_z})$  is a Hermite polynomial of order  $n_{zi}$  in the variable  $\tilde{z}\sqrt{\gamma_z}$ . The form of the basis functions  $\phi_{n_{xi}}(\tilde{x})$  and  $\phi_{n_{yi}}(\tilde{y})$  can be easily deduced from Eq. (5). Upon substituting Eq. (4) in Eq. (3), then multiplying both sides with another basis function  $\Phi_j(\tilde{x}, \tilde{y}, \tilde{z})$  and integrating with respect to  $\tilde{x}$ ,  $\tilde{y}$ , and  $\tilde{z}$  the time-independent GPE is converted into an eigenvalue problem[18]

$$\hat{F}\hat{C} = \tilde{\mu}\hat{C}, \quad (6)$$

where  $\hat{C}$  represents the column vector containing expansion coefficients  $C_i$ 's as its components, and the elements of the matrix  $\hat{F}$  are given by

$$\hat{F}_{i,j} = E_i \delta_{i,j} + V_{i,j}^{\text{anh}} + g \sum_{k,l=1}^{N_{\text{basis}}} \tilde{J}_{i,j,k,l} C_k C_l. \quad (7)$$

Above

$$E_i = \left(n_{xi} + \frac{1}{2}\right) + \left(n_{yi} + \frac{1}{2}\right)\gamma_y + \left(n_{zi} + \frac{1}{2}\right)\gamma_z, \quad (8)$$

$V_{i,j}^{\text{anh}}$  are the matrix elements of the anharmonic term in the confining potential, and  $\tilde{J}_{i,j,k,l}$  is the boson-boson repulsion matrix. For anharmonic potentials which can be written as polynomials in  $x$ ,  $y$ , and  $z$ ,  $V_{i,j}^{\text{anh}}$  can be computed

quite easily, while  $\tilde{J}_{i,j,k,l}$  can be written as a product of three submatrices corresponding to the three Cartesian directions[8]

$$\tilde{J}_{i,j,k,l} = J_{n_{xi}n_{xj}n_{xk}n_{xl}} J_{n_{yi}n_{yj}n_{yk}n_{yl}} J_{n_{zi}n_{zj}n_{zk}n_{zl}}. \quad (9)$$

It can be shown that the elements of submatrices  $J$  can be written in the form

$$J_{n_i n_j n_k n_l} = \int_{-\infty}^{\infty} d\xi \phi_{n_i}(\xi) \phi_{n_k}(\xi) \phi_{n_j}(\xi) \phi_{n_l}(\xi) \quad (10)$$

where  $\phi_{n_i}(\xi)$ 's are the harmonic oscillator basis functions of Eq. (5). Integrals involved in Eq. (10) can be computed numerically using the methods of Gaussian quadrature[11,16], or analytically[8] using the formulas derived by Busbridge[19]. In the present work, we have used this analytical expression—derived in the appendix for the sake of completeness—to compute the values of  $J$  integrals.

The eigenvalue problem of Eq.(6) has to be solved selfconsistently. In our program, for fixed values of  $N$ , this equation can be solved for  $\tilde{\mu}$  and  $\hat{C}$  using either the iterative diagonalization common in quantum chemistry[18], or the steepest-descent approach as used by Dalfovo and Stringari[9]. In both the approaches, the onset of self-consistency is signalled once the energy per particle of the condensate converges to within a user-specified threshold. This approach is different from that of Edwards *et al.*[8] where they solved Eq. (6) for  $N$ , using fixed values of  $\tilde{\mu}$ .

For the case of relatively small particle number, *i.e.*, for a weakly interacting system, it does not matter what is the nature of starting guess for the condensate orbital for initiating the SCF cycles. However, for the case of systems with large particle number, the convergence obtained is very slow (if at all), in case the starting condensate is taken to be the ground state of the harmonic trap. In such cases, the convergence is easily obtained if the starting guess for the condensate is taken to be of the Thomas-Fermi form, obtained by setting the kinetic energy term in Eq. 3 to zero

$$|\tilde{\psi}_{TF}(\tilde{\mathbf{r}})|^2 = \frac{\tilde{\mu}_{TF} - \frac{1}{2}(\tilde{x}^2 + \gamma_y^2 \tilde{y}^2 + \gamma_z^2 \tilde{z}^2)}{g}, \quad (11)$$

where the Thomas-Fermi chemical potential  $\tilde{\mu}_{TF}$  is given by

$$\tilde{\mu}_{TF} = \frac{\hbar\omega_x}{2} \left( \frac{15Na\gamma_y\gamma_z}{a_x} \right)^{2/5}. \quad (12)$$

In our program, we can also compute the Shannon entropy associated with the condensate. The Shannon mixing entropy, for a general ensemble, is defined as[20]

$$S = - \sum_i P_i \log P_i, \quad (13)$$

where  $P_i$  is the probability for a system to be in the  $i$ -th state. Of course, in the present case, we do not have a thermodynamic system in which the mixing of various states will take place due to thermal fluctuations driven by its finite temperature. Thus, the question is as to how to define Shannon entropy for the present system, which is essentially being treated as a zero-temperature quantum mechanical system. For the purpose we adopt an information theoretic point-of-view, and define the probability  $P_i$  as

$$P_i = |C_i|^2. \quad (14)$$

where  $C_i$  are the expansion coefficients of various SHO eigenstates in the expression for the condensate wave function of Eq. (4). In this picture, ground state of the condensate is seen as a statistical mixture of the various eigenstates of SHO, with the mixing probability  $P_i$ . It is important to realize that the reason behind this mixing of states is the inter-particle interaction in the condensate, because, in its absence, the condensate will be in the ground state of the SHO ( $C_i = \delta_{1,i}$ ) leading to  $S = 0$ . Thus, in a sense, entropy defined as per Eqs. (13) and (14) is a measure of inter-particle interactions in the system. Because, stronger the inter-particle interactions, the condensate will be a mixture of larger number of states, leading to a larger entropy. From an information-theoretic point-of-view larger entropy implies loss of information about the system, because, in such a case, the system is a mixture of a larger number of states. The point to be remembered, however, is that this information loss is being driven by the inter-particle interactions in the system while the corresponding information loss in a thermodynamic system is driven by its finite temperature, and the thermal fluctuations caused by it. In various contexts, other authors have also computed and discussed the information entropy associated with interacting quantum systems[21,22,23].

### 3 Description of the program

In this section we briefly describe the main program and various subroutines which constitute the entire module. All the subroutines, except for the diagonalization subroutine taken from EISPACK[24], have been written in the Fortran 90 language.

#### 3.1 Main Program OSCL

The main program is called OSCL, and its task is to read all the input information, and, among other things, fix the dimensions of various arrays. All the arrays needed in the program are dynamically allocated either in the main program, or in some of the subroutines. By utilizing the dynamic array allocation

facility of the Fortran 90 language, we have made the program independent of the size of the calculations undertaken. Because of this, the program needs to be compiled only once, and will run until the point the memory available on the computer is exhausted. Besides reading all the necessary input, program OSCL calls various subroutines in which different tasks associated with the calculation are performed.

### 3.2 *XMAT\_0*

*XMAT\_0* is a small subroutine whose job is to compute the matrix elements of the position operator in harmonic oscillator units, with respect to the basis set of a one-dimensional SHO. This routine is called from the main program OSCL, and results are stored in a two-dimensional array called *xmatrix*.

### 3.3 *Basis Set Generation*

The calculations are performed using a basis set of a three-dimensional SHO consistent with the symmetry of the system. The basis set to be used is generated by calling one of the following three routines: (a) for a spherical condensate (complete isotropy) routine *BASGEN3D\_ISO* is used, (b) for a cylindrical condensate routine *BASGEN3D\_CYL* is called, and (c) the basis set for a completely anisotropic condensate is generated using the routine *BASGEN3D\_ANISO*. In all the cases the basis functions are arranged in the ascending order of their harmonic oscillator energies and, if needed, a heap sort routine called *HPSORT* is used to achieve that. All these subroutines have the option of imposing parity symmetry on the basis set if the potential has that symmetry. This leads to a substantial reduction in the size of the basis set in most cases.

### 3.4 *HAM0\_3D*:

This subroutine is called from the main program OSCL and its purpose is to generate the matrix elements of the noninteracting (one-particle) part of the condensate Hamiltonian. If the condensate is confined in a perfectly harmonic trap, one-particle part of the Hamiltonian is trivial. However, for the case where the trap potential is anharmonic, the potential matrix elements are generated from the position operator matrix elements  $xmatrix(i, j)$  mentioned above.



### 3.5 *BEC\_DRV*

Subroutine *BEC\_DRV* is called from the main program *OSCL*, and as its name suggests, it is the driver routine for performing calculations of the condensate using the time-independent GPE. Apart from allocating a few arrays, the main task of this routine is to call either: (a) routine *BOSE\_SCF* meant for solving for the condensate wave function using the iterative-diagonalization-based SCF approach, or (b) routine *BOSE\_STEEP* used for solving for the condensate wave function using the steepest-descent approach of Dalfovo and Stringari[9].

### 3.6 *BOSE\_SCF*

This subroutine solves the time-independent GPE in a self-consistent manner using an iterative diagonalization approach. Its main tasks are as follows:

- (1) Allocate various arrays needed for the SCF calculations
- (2) Setup the starting orbitals. For this the options are: (i) diagonalize the one-particle part of the Hamiltonian, (ii) use the Thomas-Fermi orbitals, or (iii) use the orbitals obtained in a previous run.
- (3) Perform the SCF calculations. For the purpose, the two-particle integrals  $\tilde{J}_{i,j,k,l}$  (cf. Eq. (9)) are calculated on the fly during each iteration using the formulas derived in the appendix. In other words the storage of these matrix elements is completely avoided, thereby saving substantial amount of memory and disk space. This approach is akin to the “direct SCF” approach utilized in quantum chemistry. Permutation symmetries of indices  $i$ ,  $j$ ,  $k$ , and  $l$  are utilized to reduce the number of integrals evaluated. Moreover, the evaluation of an integral is undertaken only if it is found to be nonzero as per the symmetry selection rules. The integrals in question are evaluated in a subroutine called *JMNPQ\_CAL*. The  $\hat{F}$  matrix constructed in each iteration is diagonalized through a Householder diagonalization routine called *HOUSEH*, which is from the *EISPACK* package of routines[24], and is written in Fortran 77.
- (4) The chemical potential and the condensate wave function obtained after every iteration are written in various data files so that the progress of the calculation can be monitored.

### 3.7 *BOSE\_STEEP*

Alternatively, the condensate wave function and the chemical potential can be obtained using the subroutine *BOSE\_STEEP* which, instead of the iterative

diagonalization approach, utilizes the steepest-descent approach to achieve convergence, starting from a given starting orbital. In this approach, as outlined by Dalfovo and Stringari[9], the starting orbitals are evolved towards the true orbitals in small imaginary time steps by repeated application of the Hamiltonian, i.e., the  $\hat{F}$  operator. Here, the main computational step is the multiplication of a column vector by a matrix, which in the present version of the program is achieved by a call to the Fortran 90 intrinsic function MATMUL. However, one could certainly try to improve upon this by developing a subroutine which can utilize the symmetric nature of the Fock matrix. Apart from this, rest of the actions performed in this subroutine are identical to those of BOSE\_SCF.

### 3.8 THOMAS\_FERMI

This subroutine is invoked either from the subroutine BOSE\_SCF or from BOSE\_STEEP in case the SCF calculations are to be initiated by assuming Thomas-Fermi form of the starting orbitals. Upon invocation, this subroutine directly constructs the operator  $\hat{F}$  corresponding to the Thomas-Fermi orbitals. In this case, the  $\mathbf{r}$ -space integration is performed using a trapezoidal-rule-based scheme on a three-dimensional Cartesian grid.

### 3.9 ENTROPY

This subroutine is called if the entropy of the condensate needs to be computed with respect to the Harmonic oscillator basis functions, as per Eqs. 13 and 14. It is a very small subroutine with a straightforward implementation.

### 3.10 COND\_PLOT

This subroutine computes the numerical values of the condensate wave function for a user-specified set of points in space. The numerical values of the Hermite polynomials needed for the purpose are computed using the subroutine HERMITE, described below.

### 3.11 HERMITE

This subroutine computes the values of the Hermite polynomial  $H_n(x)$  for a set of user specified values of  $x$ , and order  $n$ . Fast computation of polynomials

is achieved by using initializations  $H_0(x) = 1$ ,  $H_1(x) = 2x$ , and the recursion relation  $H_{n+1}(x) = 2xH_n(x) - 2nH_{n-1}(x)$ .

## 4 Installation

All the files needed to install and run the program are kept in the gzipped, tarred archive `bose.tar.gz`. It consists of: (a) All the Fortran files containing the main program (file `osc1.f90`), and various subroutines, called by the main program, (b) four versions of Makefiles which can be used for compiling the code on various Linux/Unix systems, and (c) several sample input and output files in a subdirectory called `Examples`. The program was developed on Pentium 4 based machine running Redhat Fedora core 1 operating system using noncommercial version of the Intel Fortran compiler version 8.1. However, it has also been verified that it runs on Sun Solaris Sparc based systems, Compaq alpha (now HP alpha) based systems running True Unix, and IBM Power PC systems running AIX. For these systems, the Fortran 90 compilers supplied with those operating systems were used. In order to install and compile the program, following steps need to be followed:

- (1) Uncompress the program files in a directory of user's choice using the command `gunzip bose.tar.gz` followed by `tar -xvf bose.tar`.
- (2) Verify that the four makefiles `Makefile_linux`, `Makefile_solaris`, `Makefile_alpha`, and `Makefile_aix` are present. Copy the suitable version of the make file to the file `Makefile`. For example, if the system is a Sun Solaris Sparc system, issue the command `cp Makefile_solaris Makefile`.
- (3) Now issue the command `make` which will initiate the compilation. If everything is successful, upon completion `bin` directory of your account will have the program execution file `bose.x`. If your account does not have a directory named `bin`, you will have to either create this directory, or modify the `Makefile` to ensure that the file `bose.x` is created in the directory of your choice.
- (4) If the `bin` directory is in your path, try running the program using one of the sample input files located in the subdirectory `Examples`. For example, by issuing the command `bose.x < bec_iso.dat > x.out` one can run the program for an isotropic trap and the output will be written in a file called `x.out`. This should be compared with the supplied file `bec_iso.out` to make sure that results obtained agree with those of the example run.

Additionally, a file called `README` is also provided which lists and briefly explains all the files included in the package. Although we have not investigated the installation of the program on operating systems other than Linux/Unix, we do not anticipate any problems with such operating systems.

#### 4.1 *Input Files*

In order to keep the input process as free of errors as possible, we have adopted the philosophy that before each important input cards, there will be a compulsory comment line. It is irrelevant as to what is written in the comment lines, but, by writing something meaningful, one can keep the input process transparent. The input quantities following the comment line have to be in free format, with the restriction that the ASCII input cards should be in uppercase letters. Because of the use of comment lines, the input files are more or less self explanatory. In the sample input files, we have started all the comment lines with the character #. A sample input file corresponding to a cylindrical trap potential is listed below

```
#Type of oscillator

CYLINDRICAL

# NXMAX, NYMAX, NZMAX

10, 8

# NO. OF TERMS IN THE ANHARMONIC POTENTIAL

0

# OMEGAX, OMEGAY, OMEGAZ, JILA parameters

1.0, 2.8284271

# Type of SCF equation

GP

# No. of particles

1000

# Scattering Length, JILA Rb87

4.33d-3

# SCF convergence threshold, Maximum # of allowed iterations.

1.d-8, 1000

# Whether Parity is a good quantum number or not
```

```

PARITY

# Method for calculations

SCF

# Starting orbitals

SHO

# Whether orbital Mixing will be done

FOCKMIX

0.4

# Whether orbital plots needed

PLOT

-5.0,5.0,0.05

1

1,0,0

# Entropy Calculation

ENTROPY

1,1

```

Next we describe the input cards one by one.

- (1) First card is an ASCII card describing the type of trap potential. Options are: ISOTROPIC, CYLINDRICAL, or ANISOTROPIC.
- (2) Second card specifies the maximum quantum numbers of the basis functions to be included for various directions. For an isotropic trap one entry is needed ( $n_x = n_y = n_z$ ), for cylindrical trap, two entries are needed ( $n_x = n_y$  and  $n_z$ ), while for an anisotropic oscillator three entries are needed ( $n_x, n_y, n_z$ ). These numbers eventually determine the total number of basis functions  $N_{basis}$  used to expand the condensate as per Eq. 4.
- (3) Third card deals with the anharmonic terms in the trap potential. Any potential of the form  $\sum_{i=1}^{N_{anh}} C_i x_i^{m_i^x} y_i^{m_i^y} z_i^{m_i^z}$  can be added to the Harmonic trap potential. The first entry here is  $N_{anh}$  after which  $N_{anh}$  entries consisting of  $\{C_i, m_i^x, m_i^y, m_i^z\}$  are given. In the example input, no anhar-

monicity was considered, thus  $N_{anh}$  has been set to zero.

- (4) Fourth card deals with the trap frequencies with the convention that  $\omega_x = 1$ , and rest of the frequencies measured in the units of  $\omega_x$ . The example input corresponds to the trap frequencies of the JILA experiment with  $\omega_x = \omega_y = 1$ ,  $\omega_z = 2.284271$ .
- (5) Fifth card specifies which mean-field equation is to be solved. Options are **GP** for the Gross-Pitaevskii equation, and **HF** for the Hartree-Fock equation.
- (6) Sixth card reads the total number of bosons in the trap.
- (7) Seventh card is the value of the  $s$ -wave scattering length in the Harmonic oscillator units.
- (8) Eighth card inputs the convergence threshold, followed by the maximum number of iterations allowed to achieve convergence.
- (9) Ninth card specifies whether parity should be treated as a good quantum number or not. Options are **PARITY** and **NOPARITY**. If the trap potential is invariant under the parity operation, use of this card leads to a tremendous reduction in the size of the basis set needed to solve for the condensate wave function.
- (10) Tenth card specifies as to which method is to be used for solving the mean-field equations. Options are **SCF** corresponding to the iterative diagonalization method, and **STEEPEST-DESCENT** corresponding to the use steepest-descent method of Dalfovo and Stringari[9]. In case one opts for the steepest-descent approach, the size of the time step to be used in the calculations also needs to be specified.
- (11) Eleventh card specifies as to what sort of starting guess for the condensate should be used to start the solution process. Valid options are **SHO** corresponding to the simple-harmonic oscillator ground state and **THOMAS-FERMI** corresponding to the Thomas-Fermi form of the condensate.
- (12) It has been found that in several difficult cases, convergence can be achieved if one utilizes the techniques of Fock matrix mixing or condensate orbital mixing[9,10]. Valid options are (a) **FOCKMIX** for Fock matrix mixing (b) **ORB MIX** for condensate mixing, (c) Any other ASCII entry such as **NOMIX** for neither of these options. In case options (a) or (b) are chosen, one needs to specify the parameter  $xmix$  quantifying the mixing according to the formula

$$R^{(i)} = xmix R^{(i)} + (1 - xmix) R^{(i-1)},$$

where  $R^{(i)}$  is the quantity under consideration in the  $i$ -th iteration. Thus, if Fock matrix mixing has been opted,  $xmix$  specifies the fraction of the new Fock matrix in the total Fock matrix in the  $i$ -th iteration.

- (13) This is the penultimate card which decides whether the user wants the numerical values of condensate wave function along user specified set of data points, such that the condensate could be plotted as a function of

spatial coordinates. Keyword PLOT means that the answer is in affirmative while any other option such as NOPLOT will disable the numerical computation of the condensate. If the keyword PLOT has been supplied as in the example input, further data  $rmin$ ,  $rmax$ ,  $dr$  is specified next which determines the starting position, ending position, and the step size for generating the points on which the condensate is to be computed. After these values, we need to specify variable  $ndir$  which is the number of directions along which the condensate needs to be computed. Finally,  $ndir$  Cartesian directions have to be specified. The example input file instructs the program to compute the value of the condensate along the  $x$  axis, for  $-5.0 \leq x \leq 5.0$ , in the steps of 0.05.

- (14) Final card specifies whether one wants to compute the mixing entropy. Valid options are ENTROPY and any other entry such as NOENTROPY. If one opts for entropy calculation, one can do so for a whole range of eigenfunctions specified by their lower bound and the upper bound. Entry 1, 1 specifies that entropy of only the ground state needs to be computed.

#### 4.2 Output file

Apart from the usual information related to various system parameters, the most important information that an output file contains is the approach (or lack thereof) to convergence of the calculations as far as the chemical potential is concerned. Besides that, any other computed quantity such as the entropy is also listed in the output file. The important portions of the output file, corresponding to the input file discussed in the previous section, are reproduced below. The complete sample output file is called `bec_cyl_jila.out`, and is included in the tar archive.

SCF iterations begin

Starting chemical potential= 2.4142135

| Iteration # | Chem. Pot. | Energy/particle | Energy-Converg. |
|-------------|------------|-----------------|-----------------|
| 1           | 3.876643   | 5.3193762       | 5.3193762       |
| 2           | 4.271632   | 4.0689872       | -1.2503890      |
| 3           | 4.517259   | 3.8580062       | -0.2109810      |
| 4           | 4.619476   | 3.8439807       | -0.0140255      |
| 5           | 4.689213   | 3.8418453       | -0.0021354      |

|    |          |           |            |
|----|----------|-----------|------------|
| 6  | 4.720534 | 3.8413295 | -0.0005159 |
| 7  | 4.743576 | 3.8411720 | -0.0001575 |
| 8  | 4.753914 | 3.8411212 | -0.0000508 |
| 9  | 4.761791 | 3.8411040 | -0.0000172 |
| 10 | 4.765292 | 3.8410982 | -0.0000059 |
| 11 | 4.768022 | 3.8410961 | -0.0000020 |
| 12 | 4.769223 | 3.8410954 | -0.0000007 |
| 13 | 4.770177 | 3.8410951 | -0.0000003 |
| 14 | 4.770592 | 3.8410950 | -0.0000001 |
| 15 | 4.770927 | 3.8410950 | 0.0000000  |
| 16 | 4.771071 | 3.8410950 | 0.0000000  |
| 17 | 4.771189 | 3.8410950 | 0.0000000  |

Convergence achieved on the BEC ground state

| Eigenstate # | Information Entropy |
|--------------|---------------------|
|--------------|---------------------|

|   |           |
|---|-----------|
| 1 | 0.7477159 |
|---|-----------|

The contents of the output file listed above are self-explanatory. It basically shows that after seventeen iterations, the total energy per particle of the condensate converges to the value 3.841095, leading to the chemical potential value of 4.771. Additionally, the entropy of the condensate is computed to be 0.744771.

In addition to the above mentioned main output file, there is another output file created in the ASCII format which contains the condensate orbital obtained at the end of each iteration. This file is written in the logical unit 9, and is named `orbitals.dat`. When a new run is started, the program always looks for this file and tries to use the condensate solution present there to start the iterations. In other words, condensate solution present in `orbitals.dat` is used to restart an old aborted run. If some incompatibility is found between the condensate solution, and the present run, the solution in the `orbitals.dat` is ignored and a new run is initiated. Thus, if one wants to start a completely new run, any old `orbitals.dat` file must first be deleted.



## 5 Convergence Issues

In this section we compare the convergence of our results with respect to the size of the basis set used. We also compare the convergence properties of different iterative approaches aimed at obtaining the condensate solutions.

### 5.1 Convergence with respect to the basis set

Before treating the results obtained as the true results, one must be sure as to convergence properties with respect to the size of the basis set. This aspect of the calculations is explored in the present section by means of two examples corresponding to condensates in spherical and cylindrical traps, respectively, with fifteen hundred ( $N = 1500$ ) bosons each.

First we discuss the case of the condensate in an isotropic trap, results for which are presented in table 1. The value of the scattering length used in the calculations is listed in the caption of the table. For this case, only one value specifying the largest quantum number  $nmax$  for the basis functions, needs to be specified. It is obvious from the table that the results which have converged to three decimal places both in the chemical potential and the entropy require  $nmax = 8$ , leading to the total number of basis functions  $N_{basis} = 35$ . This means that the size of the Fock matrix diagonalized during the iterative diagonalization is  $35 \times 35$ , which is computationally very inexpensive. It is also obvious from the table that in order to get four decimal place convergence, we only need to use  $nmax = 10$  corresponding to a  $56 \times 56$  Fock matrix, whose diagonalization can also be carried out quite fast.

Similar results for the condensate in a cylindrical trap corresponding to the JILA parameters[25] are presented in table 2. Because of the anisotropy of the trap, the convergence is to be judged with respect to two parameters  $nxmax$  deciding the highest quantum number of the basis functions for  $x$ - and  $y$ -directions, and  $nzmax$  the corresponding number for the  $z$ -direction. We will first try to understand the convergence properties using a few heuristic arguments. In the JILA experiment[25] the trap frequency in the  $z$ -direction  $\omega_z$  was more than twice the value of the trap frequencies in the  $x$ - and  $y$ -directions,  $\omega_x$  and  $\omega_y$ . Therefore, due to inter-particle repulsion, the condensate will be much more delocalized along the  $x/y$ -directions, as compared to the  $z$ -direction. This means that, in order to achieve convergence, one would expect to use higher-energy basis functions in the  $x/y$ -directions, as compared to the  $z$ -direction. In other words, at convergence  $nxmax > nzmax$ . And when we examine table 2, we find that this is indeed the case. We notice that the three-decimal place convergence in both the chemical potential, and the entropy,

is obtained for  $nxmax = 8$  and  $nzmax = 6$ , although the data presented in the table covers a much larger range of parameters. Thus, we conclude that reasonably accurate values of various physical quantities can be obtained with basis sets of modest sizes, both for the isotropic as well as for the cylindrical condensates.

## 5.2 Comparison of different numerical approaches

As mentioned earlier, our program can solve the GP equation using two numerical approaches: (a) iterative diagonalization (ID) of the Fock matrix, and (b) steepest-descent (SD) method of Dalfovo *et al.*[9]. In the previous sections, all the presented results were obtained by the ID method. In the present section, we would like to present results based upon the steepest-descent approach, and compare them to those obtained using the iterative diagonalization method. We present our results for the cylindrical trap corresponding to the JILA parameters[25], with an increasing number of particles in table 3. Obviously, the numerical solution of the GP equation becomes increasingly difficult as the number of particles in the condensate grows, because of the increased contribution of the inter-particle repulsion. Therefore, it is very important to know as to how various numerical approaches perform as  $N$  is gradually increased.

As the results presented in the table suggest that for smaller values of  $N$ , neither of the two approaches have any problems achieving convergence, and the results obtained were found to be in agreement with each other to three decimal places for the basis set used. We found that in most of the cases, the ID approach worked only when Fock-matrix mixing used. Although, we managed to achieve convergence for the cases depicted in table 3 with the ID method; however, as the number of bosons in the condensate grows further, the convergence becomes slow and difficult to achieve by this method, a fact also emphasized by Schneider and Feder[11]. On the other hand, the SD approach did not have any convergence problems for the cases we investigated. As depicted in table 3, the SD approach led to convergence both with the SHO starting orbital, as well as the Thomas-Fermi starting orbital. However, for larger values of  $N$ , the use of Thomas-Fermi solution as the starting guess for the condensate, will lead to much faster convergence with this approach. Thus, we conclude that: (a) For smaller values of  $N$ , both the ID as well as the SD methods will lead to convergence, and (b) for really large values of  $N$ , the convergence is guaranteed only with the SD method. In the SD method the main computational operation is the multiplication of a vector by a matrix, which will be significantly faster as compared to the matrix diagonalization procedure needed by the ID method for calculations involving large basis sets. Thus, for calculations involving large basis sets, SD method will be faster as compared to the ID method. Therefore, all things considered, we believe that

the SD method is the more robust of the two possible approaches.

## 6 Example Runs

In this section we report the results of our calculations for a variety of trap parameters, and compare our results with those published by other authors. We also study the behavior of the Shannon entropy of the condensate with respect to the number of particles it contains. Additionally, we also present our results for the cases of anharmonic traps.

### 6.1 Comparison with other works

In this section we present the results of several calculations performed on both isotropic and the cylindrical traps, and compare them to the results obtained by other authors. Several authors have performed such calculations, however, for the sake of brevity, we restrict our comparisons mainly to the works of Bao and Tang[15] for the spherical condensate, and to the results of Dalfovo and Stringari[9] for the cylindrical condensate.

Recently, using finite-element based approach, Bao and Tang[15] performed calculations for condensates on a variety of harmonic traps, and presented results as a function of the interaction parameter  $\kappa = \frac{4\pi a N}{a_x}$ . In table 4 our results for the chemical potentials of condensates in isotropic traps corresponding to increasing values of  $\kappa$  are compared with those reported by Bao and Tang[15]. The agreement between the results obtained by two approaches is exact to the decimal places reported by Bao and Tang[15]. Note that the aforesaid agreement was obtained for rather modest basis set sizes, and calculations were completed on a personal computer in a matter of minutes.

Next we discuss the results obtained for a cylindrical trap corresponding to JILA parameters[25] for an increasing number of bosons. Our results are presented in table 5, where they are also compared to the results of Dalfovo and Stringari obtained using a finite-difference based approach[9]. The agreement between our results and those of Dalfovo and Stringari is virtually exact for all their reported calculations[9]. Again, the noteworthy point is that this level of agreement was obtained with the use of modest sized basis sets, and the computer time running into a few minutes.

Thus, the excellent agreement between our results, and those obtained by other authors using different approaches, gives us confidence about the essential correctness of our methodology. Now the question arises, will this numer-

ical method work for values of the interaction parameter  $\kappa$  which are much larger than the ones considered here. The encouraging aspect of the approach is that for none of the larger values of  $\kappa$  which we considered did we experience a numerical breakdown of the approach. It is just that for larger values of  $\kappa$ , the total number of basis functions needed to achieve convergence on the chemical potential will be larger as compared to the smaller  $\kappa$  cases. This, of course, will also lead to an increase in the CPU time needed to perform converged calculations. For example, for the case of the spherical trap considered in table 4, when we doubled  $\kappa$  to the value 6274, we needed to use basis functions corresponding to  $nmax = 20$  with  $N_{basis} = 286$  to achieve two-decimal places convergence in the chemical potential. For  $\kappa = 9411$ , to achieve similar convergence, these numbers increased to  $nmax = 24$  and  $N_{basis} = 455$ . Finally, when  $\kappa$  was increased to 15685, the corresponding numbers were  $nmax = 28$  and  $N_{basis} = 680$ , with the CPU time running into several hours. For the cylindrical trap (cf. table 5), for  $N = 20000$  bosons ( $\kappa = 1088.2$ ) the convergence was achieved in a matter of minutes with  $nxmax = 14$ ,  $nzmax = 8$  and  $N_{basis} = 180$ . When the number of bosons in the trap was doubled such that  $\kappa = 2176.4$ , similar level of convergence on the chemical potential was obtained with  $nxmax = 18$ ,  $nzmax = 8$  and  $N_{basis} = 275$ . Even with much larger values of  $\kappa$  ( $> 30000$ ) both for the spherical, and the cylindrical traps, we did not encounter any convergence difficulties when the calculations were performed with the modest sized basis sets mentioned earlier. But it was quite obvious that, to obtain highly accurate values of chemical potentials for such cases, one will have to use basis sets running into thousands which will make the calculations quite time consuming.

At this point, we would also like to compare our approach to that of Schneider and Feder[11], who used a DVR based technique to obtain accurate solutions of the time-independent GPE. In the DVR approach the basis functions are the so-called “coordinate eigenfunctions”, which, in turn, are assumed to be linear-combinations of other functions such as the SHO eigenstates, or the Lagrange interpolating functions[11]. Thus in the DVR approach of Schneider and Feder[11], the SHO eigenstates are used as intermediate basis functions, and not as primary basis functions as is done in our approach. Using this approach, coupled with the “direct-inversion in the iterative space” (DIIS) method, Feder and Schneider managed to obtain accurate solutions for anisotropic condensates for quite large values of the interaction parameter  $\kappa$ [11]. However, the price to be paid for this accuracy was the use of a very large basis set consisting of several thousands of basis functions[11] even for rather small values of  $\kappa$ .

Finally, we present the plots of the condensates in a spherical trap, for increasing values of  $N$ , in Fig. 1. As expected, the calculations predict a depletion of central condensate density, and corresponding delocalization of the condensate, with increasing  $N$ . The results presented are in excellent agreement

with similar results presented by various other authors[9,15]. Moreover, if we compare the value of the condensate at the center of the trap ( $|\psi(0,0,0)|$ ) for the isotropic trap with the published results of Bao and Tang[15], we again obtain excellent agreement for all values of  $N$ .

## 6.2 Anharmonic Potentials

Recently, several studies have appeared in the literature studying the influence of trap anharmonicities on the condensates, in light of rotating condensates, and the resultant vortex structure[26]. However, we approach the influence of trap anharmonicity from a different perspective, namely that of quantum chaos. Therefore, the anharmonicities considered here are in the absence of any rotation, and the aim is to study their influence on the ground and the excited states of the condensate. We assume the unperturbed harmonic trap to be the cylindrical one corresponding to the JILA parameters[25], and consider two types of anharmonic perturbations in the  $x - y$  plane: (a) the Henon-Heiles potential with  $V^{anh}(x, y) = \alpha(x^2y - \frac{1}{3}y^3)$ , and (b) the Fourleg potential  $V^{anh}(x, y) = \alpha x^2y^2$ , where  $\alpha$  is the anharmonicity parameter. Note that the Henon-Heiles potential reduces the circular symmetry of the cylindrical trap in the  $x - y$  plane to the triangular one (symmetry group  $C_{3v}$ ), and the fourleg potential reduces the symmetry to that of a square (group  $C_{4v}$ ). In case of Henon-Heiles potential the inversion symmetry of the cylindrical trap is also destroyed, while for the fourleg potential, it is still preserved. The Henon-Heiles potential introduces deconfinement in the trap, the Fourleg potential, on the other hand, strengthens the confinement of the original trap. Both these potentials are known to lead to chaotic behavior for higher energy states, both at the classical and quantum-mechanical levels of theories[27,28]. In a separate work communicated elsewhere, we have examined the excited states of condensates under the influence of these potentials, in order to analyze the signatures of chaotic behavior. In the present work, however, we intend only to demonstrate the capabilities of our program as far as the anharmonicity is concerned, and restrict ourselves only to the ground states of the condensates in presence of these potentials. Results of our calculations on the chemical potentials of condensates in a cylindrical trap corresponding to the JILA experiment[25], and  $N = 1000$ , are presented in table 6 as a function of anharmonicity  $\alpha$ . Corresponding plots of the condensate along the  $y$  axis are presented in Fig. 2. As far as the influence of anharmonicity on the chemical potential is concerned, from table 6 we conclude that, for a given value of  $N$ , for increasing  $\alpha$ , it increases for the Henon-Heiles potential, and decreases for the fourleg potential. Similarly, upon examining the Fig. 2, we conclude that for the Henon-Heiles potential, the central condensate density gets depleted with increasing  $\alpha$ , while the behavior in case of the fourleg potential is just the opposite. Additionally, the fact that the inversion symmetry is broken in case

of Henon-Heiles potential, is obvious from the asymmetry of corresponding condensate plots.

### 6.3 Entropy Calculations

Here we discuss the Shannon entropy of condensates in isotropic and cylindrical traps, as a function of the dimensionless strength parameter  $\kappa = \frac{4\pi a N}{a_x}$ . Since the scattering length in most of the traps is fixed, for such cases the change in  $\kappa$  can be construed as due to changes in  $N$ . In Fig. 3 we present the plots of Shannon entropy versus  $\kappa$  plots for the condensates trapped both in isotropic, as well as cylindrical traps. Although a detailed analysis of the Shannon entropy of condensates is being presented elsewhere, we make a couple of important observations: (i) For both types of traps the entropy increases as a function of  $\kappa$ . Initially, the rate of increase is quite high, but for larger values of  $\kappa$ , it settles down to a much lower value. (ii) For a given nonzero value of  $\kappa$ , the entropy of a condensate in a cylindrical trap is always larger than that of a condensate in a spherical trap. In other words, the trap anisotropy appears to increase the Shannon entropy of the system.

## 7 Conclusions

In this paper we have reported a Fortran 90 implementation of a harmonic oscillator basis set based approach towards obtaining the numerical solutions of time independent GPE. We have presented applications of our program to a variety of situations including anharmonic potentials, and in calculations of the Shannon entropy of the condensate. We also compared the results obtained from our program to those obtained by other authors, and found near-perfect agreement. Therefore, we encourage the users to apply our program to a variety of situations, and contact us in case they encounter errors. We have extensive plans for further development of our program. Some of the possible directions are: (a) extension of our approach to time-dependent GPE, allowing one to deal with condensate dynamics, (b) taking condensate rotation into account, allowing one to study the vortex phenomena, and (c) dealing with condensates with nonzero spins, i.e., the so-called spinor condensates[29]. Work along these lines is presently in progress in our group, and, upon completion, will be reported in future publications.

## A Appendix

Here our aim is to compute the two-particle integral of Eq. (10) defined as

$$J_{n_i n_j n_k n_l} = \int_{-\infty}^{\infty} d\xi \phi_{n_l}(\xi) \phi_{n_k}(\xi) \phi_{n_j}(\xi) \phi_{n_i}(\xi), \quad (\text{A.1})$$

where, in terms of the dimensionless coordinates  $\xi$ , the single particle wave function  $\phi_{n_i}(\xi)$  is given by

$$\phi_{n_i}(\xi) = \frac{1}{\sqrt{\sqrt{\pi} 2^{n_i} n_i!}} H_{n_i}(\xi) e^{-\frac{\xi^2}{2}}. \quad (\text{A.2})$$

Substituting Eq.A.2 in Eq. (10), we get

$$J_{n_i n_j n_k n_l} = \frac{1}{\pi \sqrt{2^{n_i+n_j+n_k+n_l} n_i! n_j! n_k! n_l!}} I_{n_i n_j n_k n_l}, \quad (\text{A.3})$$

where

$$I_{n_i n_j n_k n_l} = \int_{-\infty}^{\infty} e^{-2\xi^2} H_{n_i}(\xi) H_{n_j}(\xi) H_{n_k}(\xi) H_{n_l}(\xi) d\xi. \quad (\text{A.4})$$

Since Hermite polynomials have a definite parity, the integral  $I_{n_i n_j n_k n_l}$  will be nonvanishing only if the sum  $n_i + n_j + n_k + n_l$  is an even number. Now we will use a standard result for the product of two Hermite Polynomials,

$$H_m(\xi) H_n(\xi) = \sum_{k=0}^{\min\{m,n\}} 2^k k! \binom{m}{k} \binom{n}{k} H_{m+n-2k}(\xi), \quad (\text{A.5})$$

where  $\binom{m}{k}$  etc. are the binomial coefficients. Upon substituting Eq. A.5 in Eq. A.4, we obtain

$$I_{m,n,q,r} = \sum_{k=0}^{\min\{m,n\}} \sum_{l=0}^{\min\{q,r\}} 2^{k+l} k! l! \binom{m}{k} \binom{n}{k} \binom{q}{l} \binom{r}{l} \int_{-\infty}^{\infty} e^{-2\xi^2} H_{m+n-2k}(\xi) H_{q+r-2l}(\xi) d\xi. \quad (\text{A.6})$$

In order to perform the integral above, we recall the result derived by Busbridge[19]

$$\int_{-\infty}^{\infty} e^{-2\xi^2} H_m(\xi) H_n(\xi) d\xi = (-1)^{\frac{m-n}{2}} 2^{\frac{m+n-1}{2}} \Gamma\left(\frac{m+n+1}{2}\right), \quad (\text{A.7})$$

for  $m + n = \text{even}$ . Substituting this we get

$$I_{m,n,q,r} = (-1)^{\frac{m+n-p-q}{2}} 2^{\frac{m+n+p+q-1}{2}} K_{m,n,q,r}, \quad (\text{A.8})$$

where

$$K_{m,n,q,r} = \sum_{k=0}^{\min\{m,n\}} \sum_{l=0}^{\min\{q,r\}} (-1)^{l-k} k! l! \binom{m}{k} \binom{n}{k} \binom{q}{l} \binom{r}{l} \Gamma\left(\frac{m+n+q+r-2k-2l}{2} + \frac{1}{2}\right). \quad (\text{A.9})$$

Upon substituting Eqs. (A.8) and (A.9) in Eq. (A.3), we get

$$J_{m,n,q,r} = (-1)^{\frac{m+n-q-r}{2}} \frac{1}{\pi \sqrt{2(m!n!q!r!)}} K_{m,n,q,r}. \quad (\text{A.10})$$

On using the expression

$$\Gamma\left(\frac{2n+1}{2}\right) = \frac{2n!}{2^{2n} n!} \sqrt{\pi}, \quad (\text{A.11})$$

and setting  $m + n + q + r = 2t$ , we have

$$\Gamma\left(\frac{m+n+q+r-2k-2l}{2} + \frac{1}{2}\right) = \frac{(2t-2k-2l)! \sqrt{\pi}}{2^{2t-2k-2l} (t-k-l)!}. \quad (\text{A.12})$$

Upon substituting Eq. (A.12) and the values of binomial coefficients in Eq. (A.9), we have

$$K_{m,n,q,r} = \frac{\sqrt{\pi}}{2^{m+n+q+r}} m! n! q! r! \times \sum_{k,l} \frac{(-1)^{l-k} 2^{2(k+l)} (2t-2k-2l)!}{(m-k)! (n-k)! (q-l)! (r-l)! (k!) (l!) (t-k-l)!}, \quad (\text{A.13})$$

which, upon substitution in Eq. (A.10), leads to the final expression

$$J_{m,n,q,r} = \frac{(-1)^{\frac{m+n-q-r}{2}}}{2^{m+n+q+r}} \sqrt{\frac{m!n!q!r!}{2\pi}} L_{m,n,q,r}, \quad (\text{A.14})$$

where

$$L_{m,n,q,r} = \sum_{k=0}^{\min\{m,n\}} \sum_{l=0}^{\min\{q,r\}} \frac{(-1)^{l-k} 2^{2k+2l} (2t-2k-2l)!}{(m-k)! (n-k)! (q-l)! (r-l)! (k!) (l!) (t-k-l)!}. \quad (\text{A.15})$$

Expressions of Eqs. (A.14) and (A.15) have been used in the function JINTT, which is called via subroutine JMNPQ\_CAL, to compute these two-body integrals. We would like to emphasize that the series of Eq. (A.15) has terms



with alternating signs, and, therefore, is potentially unstable for large values of  $m$ ,  $n$ ,  $q$ , and  $r$ . Thus, it is crucial to use high arithmetic precision while summing the series. With the usual double-precision arithmetic (REAL\*8 variables), we found that the the series was unstable for values of  $m$ ,  $n$ ,  $q$ ,  $r$  larger than 16. To circumvent these problems, we used quadruple precision (REAL\*16 variables) in function JINTT to sum the series. Once the summation is performed, the results are converted into the double-precision format. We believe that this approach has made the two-particle integral calculation process very robust, and accurate.

## References

- [1] M. H. Anderson, J. R. Ensher, M. R. Matthews, C. E. Wieman, and E. A. Cornell, *Science* 269 (1995) 198.
- [2] C. C. Bradley, C. A. Sackett, J. J. Tollett, and R. G. Hulet, *Phys. Rev. Lett.* 75 (1995) 1687.
- [3] K. B. Davis, M.-O. Mewes, M. R. Andrews, N. J. van Druten, D. S. Durfee, D. M. Kurn, and W. Ketterle, *Phys. Rev. Lett.* 75 (1995) 3969.
- [4] For a review, see, *e.g.*, F. Dalfovo, S. Giorgini, L. P. Pitaevskii, and S. Stringari, *Rev. Mod. Phys.* 71 (1999) 463.
- [5] E. P. Gross, *Nuovo. Cimento.* 20 (1961) 454.
- [6] L. P. Pitaevskii, *Zh. Eksp. Teor. Fiz.* 40 (1961) 646.
- [7] M. Edwards and K. Burnett, *Phys. Rev. A* 51 (1995) 1382.
- [8] M Edwards, R. J. Dodd, C. W. Clark, P. A. Ruprecht and K. Burnett, *Phys. Rev. A* 53 (1996) R1950.
- [9] F. Dalfovo and S. Stringari, *Phys. Rev. A* 53 (1996) 2477.
- [10] B. D. Esry, *Phys. Rev. A* 55 (1997) 1147.
- [11] B. I. Schneider and D. L. Feder, *Phys. Rev. A* 59 (1999) 2232.
- [12] S. K. Adhikari, *Phys. Lett. A* 265 (2000) 91.
- [13] S. K. Adhikari, *Phys. Rev. E* 62 (2000) 2937.
- [14] M. L. Chiofalo, S. Succi and M. P. Tosi, *Phys. Rev E* 62 (2000) 7438.
- [15] W. Bao and W. Tang, *J. Comp. Phys.* 187 (2003) 230.
- [16] C. M. Dion and E. Cancès, *Phys. Rev. E* 67 (2003) 046706.
- [17] K. Ziegler and A. Shukla, *Phys. Rev. A* 56 (1997) 1438.

- [18] See, *e.g.*, A. Szabo and N. S. Ostlund, *Modern Quantum Chemistry: Introduction to Advanced Electronic Structure Theory* (Dover Publications, New York, 1996).
- [19] I. W. Busbridge, *J. London Math. Soc.* **23**, 135 (1948).
- [20] C. E. Shannon, *Bell System Tech. J.* **27** (1948) 379, 623.
- [21] See, *e.g.*, S. R. Gadre, *Phys. Rev. A* **30**, 620 (1984); S. R. Gadre and R. D. Bendale, *ibid.* **36**, 1932 (1987).
- [22] P. Ziesche, *Int. J. Quantum Chem.* **56**, 363 (1995).
- [23] Ch. C. Moustakidis and S. E. Massen, *Phys. Rev. B* **71**, 045102 (2005).
- [24] B. Smith, J. Boyle, J. Dongarra, B. Garbow, Y. Ikebe, V. Klema, and C. Moler, *Matrix Eigenvalues Routines, EISPACK Guide, Lecture Notes in Computer Science*, Vol. 6, Springer Verlag (1976).
- [25] These are the parameters used to describe the experiment of Anderson *et al.* on  $^{87}\text{Rb}$ [1]. They correspond to a frequency ratio  $\frac{\omega_z}{\omega_x} = \sqrt{8}$ , and the scattering length  $a = 4.33 \times 10^{-3} a_x$ . These parameters were also used by Dalfovo *et al.* in their calculations[9].
- [26] See, *e.g.*, A. L. Fetter, *Phys. Rev. A* **64** (2001) 063608.; E. Lundh, *Phys. Rev. A* **65** (2002) 043604.
- [27] R. A. Pullen and A. R. Edmonds, *J. Phys. A* **14** (1981) L319.
- [28] R. A. Pullen and A. R. Edmonds, *J. Phys. A* **14** (1981) L477.
- [29] T.-L. Ho, *Phys. Rev. Lett.* **81** (1998) 742.

Table 1

Convergence on the chemical potential and the mixing entropy of the condensate in an isotropic trap with scattering length  $a = 2.4964249 \times 10^{-3} a_x$  and number of bosons  $N = 1500$ , with respect to the basis set size.  $nmax$  is the maximum value of the quantum number of the SHO basis function in a given direction,  $N_{basis}$  is the total number of basis functions corresponding to a given value of  $nmax$ , and  $N_{iter}$  represents the total number of SCF iterations needed to achieve convergence on the condensate energy per particle. In all the calculations iterative diagonalization method, along with Fock matrix mixing with  $xmax = 0.6$ , was used. The SCF convergence threshold was  $1.0 \times 10^{-7}$ .

| $nmax$ | $N_{basis}$ | $N_{iter}$ | Chemical Potential | Entropy   |
|--------|-------------|------------|--------------------|-----------|
| 2      | 4           | 19         | 2.939116           | 0.5083669 |
| 4      | 10          | 11         | 2.915046           | 0.5387074 |
| 6      | 20          | 14         | 2.911181           | 0.5396975 |
| 8      | 35          | 14         | 2.911278           | 0.539088  |
| 10     | 56          | 15         | 2.911375           | 0.5392423 |
| 12     | 84          | 15         | 2.911346           | 0.5392770 |
| 14     | 120         | 15         | 2.911337           | 0.5392822 |
| 16     | 165         | 13         | 2.911337           | 0.5392797 |

Table 2

Convergence on the chemical potential and the mixing entropy of the condensate in a cylindrical trap with trap parameters corresponding to the JILA experiment[25], and the number of bosons  $N = 1500$ , with respect to the basis set size.  $nxmax$  is the maximum value of the quantum number of the SHO basis function in  $x$ - and  $y$ -direction,  $nzmax$  is the same number corresponding to the  $z$ -direction. Rest of the quantities have the same meaning as explained in the caption of table 1. In all the calculations iterative diagonalization, along with Fock matrix mixing with  $xmax = 0.3$ , was used. The SCF convergence threshold was  $1.0 \times 10^{-8}$ .

| $nxmax$ | $nzmax$ | $N_{basis}$ | $N_{iter}$ | Chemical Potential | Entropy   |
|---------|---------|-------------|------------|--------------------|-----------|
| 4       | 0       | 6           | 39         | 5.786323           | 0.9387124 |
| 4       | 2       | 12          | 19         | 5.421930           | 0.9383227 |
| 4       | 4       | 18          | 27         | 5.423981           | 0.9380013 |
| 6       | 0       | 10          | 31         | 5.737602           | 0.9770727 |
| 6       | 2       | 20          | 19         | 5.405221           | 0.9549194 |
| 6       | 4       | 30          | 20         | 5.405440           | 0.9545441 |
| 6       | 6       | 40          | 20         | 5.404970           | 0.9545920 |
| 8       | 0       | 15          | 21         | 5.737074           | 0.9752491 |
| 8       | 2       | 30          | 20         | 5.404605           | 0.9546530 |
| 8       | 4       | 45          | 21         | 5.404691           | 0.9542773 |
| 8       | 6       | 60          | 21         | 5.404218           | 0.9543291 |
| 8       | 8       | 75          | 21         | 5.404147           | 0.9543239 |
| 10      | 0       | 21          | 21         | 5.736935           | 0.9755365 |
| 10      | 2       | 42          | 20         | 5.404741           | 0.9544814 |
| 10      | 4       | 63          | 20         | 5.404540           | 0.9541044 |
| 10      | 6       | 84          | 20         | 5.404066           | 0.9541561 |
| 10      | 8       | 105         | 18         | 5.403994           | 0.9541508 |
| 10      | 10      | 126         | 18         | 5.403991           | 0.9541477 |
| 12      | 0       | 28          | 21         | 5.736763           | 0.9756539 |
| 12      | 2       | 56          | 20         | 5.404636           | 0.9545789 |
| 12      | 4       | 84          | 20         | 5.404436           | 0.9542004 |
| 12      | 6       | 112         | 20         | 5.403962           | 0.9542517 |
| 12      | 8       | 140         | 20         | 5.403891           | 0.9542463 |
| 12      | 10      | 168         | 20         | 5.403888           | 0.9542432 |
| 12      | 12      | 196         | 18         | 5.403888           | 0.9542428 |

Table 3

Comparison of the chemical potentials ( $\mu$ ) obtained using the iterative diagonalization (ID) technique, and the steepest-descent (SD) technique[9], for the condensates in a cylindrical trap with trap parameters corresponding to the JILA experiment[25], and a given number of bosons ( $N$ ). Quantities  $N_{iter}$ ,  $nxmax$ , and  $nzmax$  have the same meaning as in the caption of table 2, and  $\mu$  is expressed in the units of  $\hbar\omega_x$ . In the ID based calculations for  $N \leq 2000$ , SHO ground state solution was used to start the iterations, while for larger values of  $N$  the iterations were started using the Thomas-Fermi approximation. In all the cases corresponding to the ID method, Fock matrix mixing was used, with  $0.05 \leq xmax \leq 0.3$ . In the SD based calculations, the iterations were started using the Thomas-Fermi approximation, with the size of the time step being 0.02 units.

| $N$   | $nxmax$ | $nzmax$ | $N_{iter}(\text{ID})$ | $N_{iter}(\text{SD})$ | $\mu(\text{ID})$ | $\mu(\text{SD})$ |
|-------|---------|---------|-----------------------|-----------------------|------------------|------------------|
| 500   | 8       | 6       | 16                    | 62                    | 3.938611         | 3.938865         |
| 1000  | 8       | 6       | 14                    | 88                    | 4.770707         | 4.772055         |
| 1500  | 8       | 6       | 21                    | 95                    | 5.404218         | 5.405491         |
| 2000  | 12      | 8       | 23                    | 104                   | 5.931870         | 5.932878         |
| 10000 | 14      | 8       | 86                    | 99                    | 10.505267        | 10.505124        |
| 15000 | 14      | 8       | 105                   | 129                   | 12.239700        | 12.239465        |
| 20000 | 14      | 8       | 104                   | 109                   | 13.665923        | 13.665686        |

Table 4

Comparison of the chemical potentials (in the units of  $\hbar\omega$ ) obtained from our program, and those reported by Bao and Tang[15], for an isotropic trap, with increasing values of interaction parameter  $\kappa$ . The negative value of  $\kappa$  implies attractive inter-particle interactions. For the value of scattering length stated in table 1,  $\kappa = 3137.1$  corresponds to  $N = 1 \times 10^5$  bosons. Symbols  $nmax$  and  $N_{iter}$  have the same meaning as in the previous tables. For the last two calculations, SD method with a time step of 0.02 units, and Thomas-Fermi initial guess were employed. Our chemical potentials have been truncated to as many decimal places as reported by Bao and Tang[15].

| $\kappa$ | $nmax$ | $N_{basis}$ | $\mu(\text{This work})$ | $\mu(\text{Ref.}[15])$ |
|----------|--------|-------------|-------------------------|------------------------|
| -3.1371  | 14     | 120         | 1.2652                  | 1.2652                 |
| 3.1371   | 14     | 120         | 1.6774                  | 1.6774                 |
| 12.5484  | 14     | 120         | 2.0650                  | 2.0650                 |
| 31.371   | 14     | 120         | 2.5861                  | 2.5861                 |
| 125.484  | 14     | 120         | 4.0141                  | 4.0141                 |
| 627.42   | 16     | 165         | 7.2485                  | 7.2484                 |
| 3137.1   | 16     | 165         | 13.553                  | 13.553                 |

Table 5

Comparison of the chemical potentials (in the units of  $\hbar\omega_x$ ) obtained from our program, and those reported by Dalfovo and Stringari[9], for a cylindrical trap corresponding to the JILA parameters[25], with increasing number  $N$  of bosons. Symbols  $nxmax$ ,  $nzmax$ , and  $N_{iter}$  have the same meaning as in the previous tables. Calculations for  $N \geq 10000$  were performed by the SD method using Thomas-Fermi starting orbitals, a time-step of 0.02 units, and a convergence threshold of  $1.0 \times 10^{-7}$ . We have truncated our chemical potentials to as many decimal places as reported by Dalfovo and Stringari[9].

| $N$   | $nxmax$ | $nzmax$ | $N_{basis}$ | $\mu$ (This work) | $\mu$ (Ref.[9]) |
|-------|---------|---------|-------------|-------------------|-----------------|
| 100   | 8       | 6       | 60          | 2.88              | 2.88            |
| 200   | 8       | 6       | 60          | 3.21              | 3.21            |
| 500   | 8       | 6       | 60          | 3.94              | 3.94            |
| 1000  | 8       | 6       | 60          | 4.77              | 4.77            |
| 2000  | 8       | 6       | 60          | 5.93              | 5.93            |
| 5000  | 10      | 8       | 105         | 8.14              | 8.14            |
| 10000 | 10      | 8       | 105         | 10.5              | 10.5            |
| 15000 | 14      | 8       | 180         | 12.2              | 12.2            |
| 20000 | 14      | 8       | 180         | 13.7              | 13.7            |

Table 6

Influence of trap anharmonicities on the chemical potential. The table below presents results for the Henon-Heiles, and the fourleg potentials, for cylindrical trap corresponding to JILA parameters[25], with  $N = 1000$ .

| $\alpha$ | $\mu$ (Henon-Heiles) | $\mu$ (Fourleg) |
|----------|----------------------|-----------------|
| 0.00     | 4.7712               | 4.7712          |
| 0.03     | 4.7662               | 4.8261          |
| 0.06     | 4.7497               | 4.8752          |
| 0.09     | 4.7207               | 4.9202          |
| 0.12     | 4.6764               | 4.9619          |
| 0.15     | 4.6131               | 5.0009          |

Figure 1. Plots of condensates along the  $x$  axis for an isotropic trap, with an increasing number of  $N$  of bosons. The trap parameters used were the same as in the data of tables 1 and 4. Lines correspond to  $N = 100, 500, 1000, 5000,$  and  $10000,$  and are in the descending order of the central condensate density, and distances are in the units of  $a_x$ .

Fig 1: Tiwari and Shukla

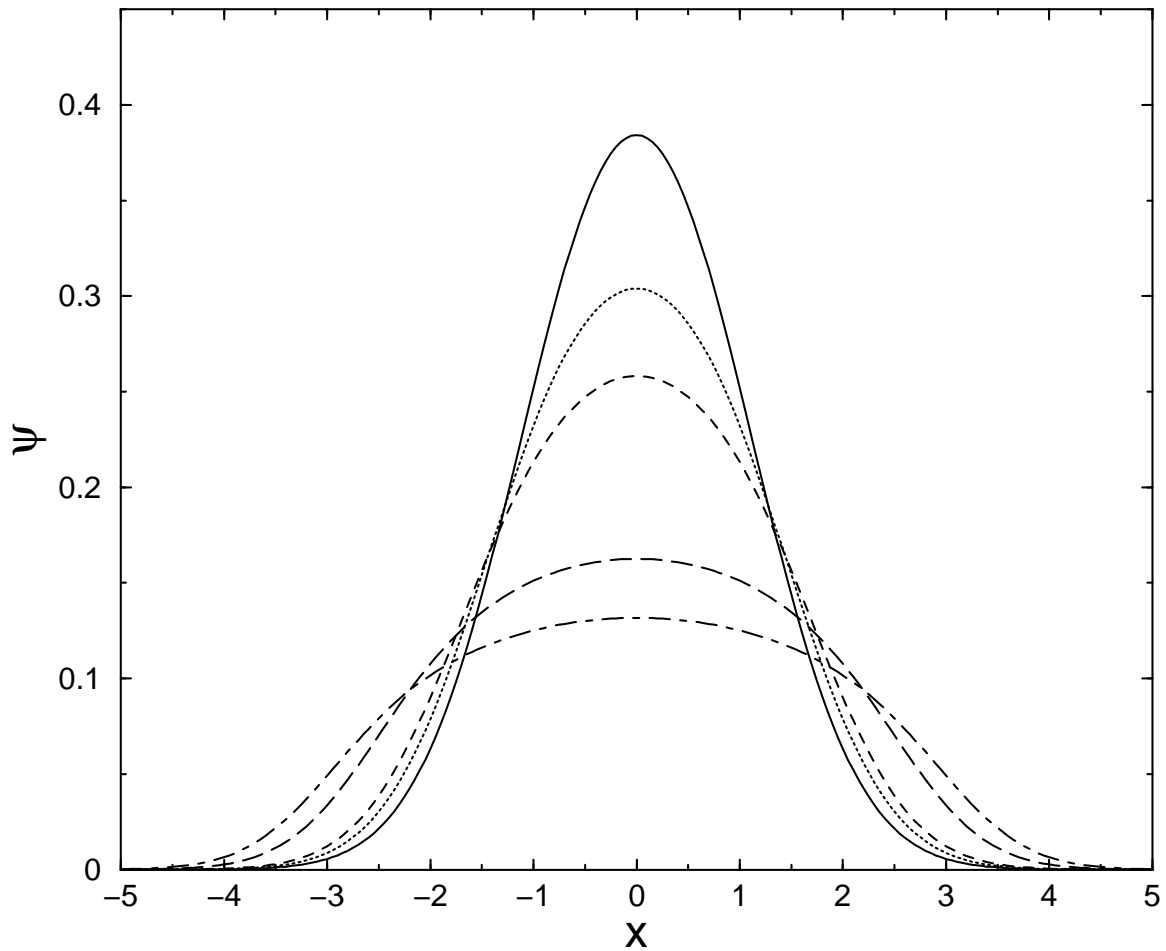


Figure 2. Influence of various types of anharmonicities on condensates in cylindrical traps with  $N = 1000$ , and scattering length corresponding to the JILA parameters[25]. The plots correspond to: (a) the Henon-Heiles potential, and (b) the Fourleg potential. In each graph, solid, dotted, and dashed lines represent values of anharmonicity parameter (see text)  $\alpha = 0.0, 0.05, \text{ and } 0.15$ , respectively. The  $y$  coordinate is measured in the units of  $a_x$ .

Fig 2: Tiwari and Shukla

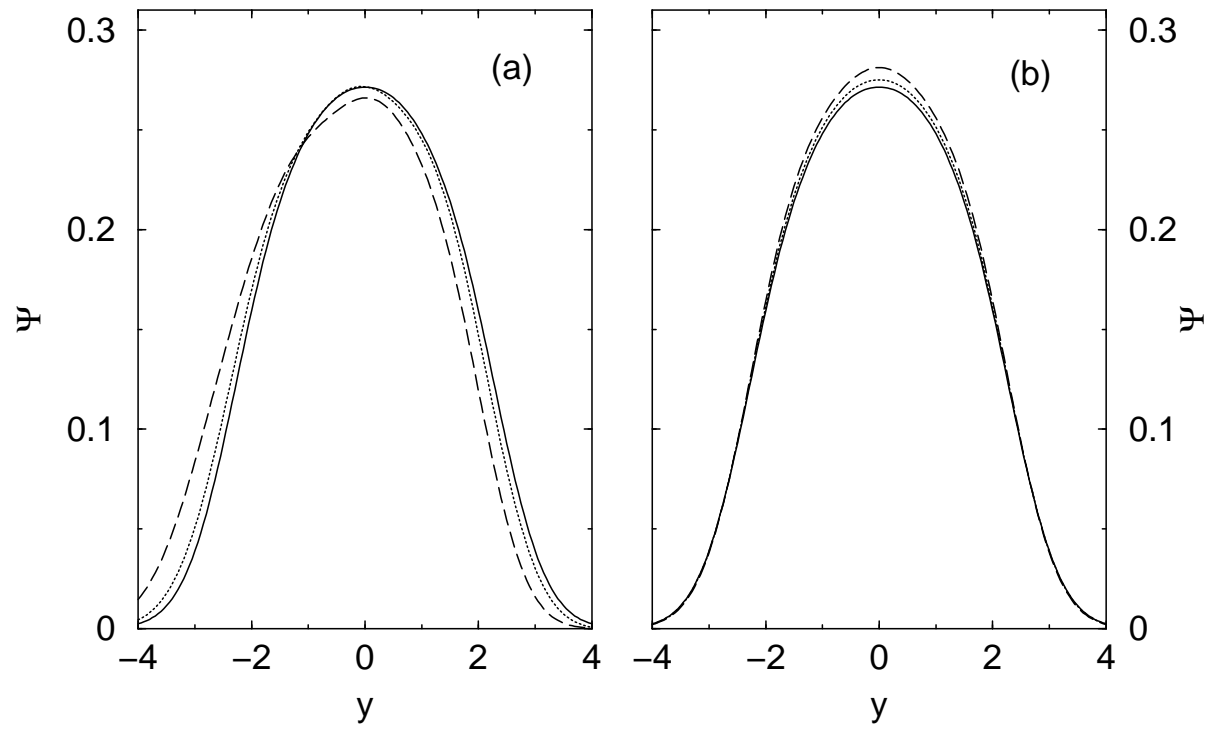




Figure 3. Plots of Shannon entropy of condensates in an isotropic trap (solid line) and cylindrical trap (dashed line), as a function of the dimensionless strength parameter  $\kappa = \frac{4\pi a N}{a_x}$ .

Fig 3: Tiwari and Shukla

